walls. Because of the symmetry of the geometry and boundary conditions, only one-half of the cavity is modeled, with a grid size of $41 \times 41 \times 21$. As reported by Reddy and Reddy,[11] two test cases of Rayleigh numbers, 10^3 and 10^4, with Prandtl number equal to unity are considered here. The variation of the temperature and the vertical component of velocity vector on the horizontal midline of the symmetry plane ($y = 0.5$ and $z = 0.5$) are plotted in Fig. 3. The solutions show very good agreement with the results of Reddy and Reddy.[11]

Turbulent Results

The problem considered here is a two-dimensional square enclosure with hot left vertical wall, cold right vertical wall, and adiabatic horizontal walls. With $Pr = 0.71$ and $Ra = 5 \times 10^{10}$, the flow inside the cavity is turbulent.[12] A grid size of 57×57 with clustering (as given in Ref. 12) is used for the computations. The contour plots for temperature and turbulent kinematic viscosity are shown in Fig. 4. The present computation is able to capture the flow features such as thermal stratification in the core of the enclosure and turbulent viscosity concentration in the vertical boundary layers as given in Ref. 12. Qualitatively the contour plots agree very well with the results shown by Henkes and Hoogendoorn.[12] The quantitative comparisons of turbulent viscosity and vertical velocity along the horizontal centerline and temperature along the vertical centerline are found to be in an acceptable range of the results in Ref. 12.

Conclusions

The pseudocompressibility approach, commonly used for isothermal cases, has been successfully applied to compute flows with natural convection for both laminar and turbulent flow situations. The results obtained by the present method compare very well with experimental and benchmark numerical solutions given in the literature, thus demonstrating the ability of pseudocompressibility method in accurately predicting flows for heat transfer problems.

References

[1]Markle, C. L., and Athavale, M., "Time Accurate Unsteady Incompressible Flow Algorithms Based on Artificial Compressibility," AIAA Paper 87-1137, 1984.

[2]Chorin, A. J., "A Numerical Method for Solving Incompressible Viscous Flow Problems," *Journal of Computational Physics*, Vol. 2, No. 1, 1967, pp. 12–26.

[3]Belov, A., Martinelli, L., and Jameson, A., "A New Implicit Algorithm with Multigrid for Unsteady Incompressible Flow Calculation," AIAA Paper 95-0049, 1990.

[4]Dreyer, J., "Finite Volume Solutions to the Unsteady Incompressible Euler Equations on Unstructured Triangular Meshes," M.S. Thesis, Mechanical and Aerospace Engineering Dept., Princeton Univ., Princeton, NJ, 1990.

[5]Chang, J. L. C., Kwak, D., Rogers, S. E., and Yang, R. L., "Numerical Simulation Methods of Incompressible Flows and an Application to the Space Shuttle Main Engine," *International Journal for Numerical Methods in Fluids*, Vol. 8, 1988, pp. 1241–1266.

[6]Rizzi, A., and Eriksson, L., "Computation of Inviscid Incompressible Flow with Rotation," *Journal of Fluid Mechanics*, Vol. 153, 1985, pp. 275–312.

[7]Farmer, J., Martinelli, L., and Jameson, A., "Fast Multigrid Method for Solving Incompressible Hydrodynamic Problems with Free Surfaces," *AIAA Journal*, Vol. 32, 1994, pp. 1175–1182.

[8]Tamamidis, P., Zhang, G., and Assanis, D. N., "Comparison of Pressure Based and Artificial Compressibility Methods for Solving 3D Steady Incompressible Viscous Flows," *Journal of Computational Physics*, Vol. 124, 1996, pp. 1–13.

[9]de Vahl Devis, G., "Natural Convection of Air in a Square Cavity: A Bench Mark Numerical Solution," *International Journal for Numerical Methods in Fluids*, Vol. 3, 1983, pp. 249–264.

[10]Kuehn, T. H., and Goldstein, R. J., "An Experimental and Theoretical Study of Natural Convection in the Annulus Between Horizontal Concentric Cylinders," *Journal of Fluid Mechanics*, Vol. 74, 1976, pp. 695–719.

[11]Reddy, M. P., and Reddy, J. N., "Penalty Finite Element Analysis of Incompressible Flow Using Element by Element Solution Algorithms," *Computer Methods is Applied Mechanics and Engineering*, Vol. 100, 1992, pp. 169–205.

[12]Henkes, R. A. W. M., and Hoogendoorn, C. J., "Comparison Exercise for Computation of Turbulent Natural Convection in Enclosure," *Numerical Heat Transfer*, Pt. B, Vol. 28, 1995, pp. 59–78.

[13]Menter, F. R., "A Comparison of Some Recent Eddy-Viscosity Turbulence Models," *Journal of Fluids Engineering*, Vol. 118, 1996, pp. 514–519.

[14]Turkel, E., "Preconditioned Methods for Solving the Incompressible and Low Speed Compressible Equations," *Journal of Computational Physics*, Vol. 72, 1987, pp. 277–298.

[15]Marvin, J. G., and Huang, G. P., "Status and Future Direction for Turbulence Modeling," *Sadhana*, Vol. 23, 1998, pp. 481–503.

Freezing Couette Flow in an Annulus with Translating Outer Sleeve

Carsie A. Hall III*
University of New Orleans, New Orleans, Louisiana 70148
Calvin Mackie†
Tulane University, New Orleans, Louisiana 70118
and
Judy A. Perkins‡
North Carolina A&T State University, Greensboro, North Carolina 27411

Introduction

INTERNAL fluid flows undergoing phase change (melting or freezing) have been the subject of research due to applications in manufacturing processes, freeze blockage of liquids in pipes, low-temperature viscometers, circular and annular thrust bearings, etc.[1,2] Typically, these fluids exhibit Newtonian as well as non-Newtonian behavior.[3,4] Analytical solutions to flows that exhibit Couette (or Couette-like) behavior such as purely shear-driven flows and near-wall turbulent flows with solid–liquid phase change have appeared sparsely in the literature. Most analytical solutions have been obtained for problems involving semi-infinite regions. For example, Huang[5] studied the transient Couette flow problem with viscous heating and used a combination of the similarity technique and Green's function to derive a closed-form solution for one-dimensional melting of a semi-infinite solid region by a hot moving wall.

In the present Note, an analytical solution is presented for one-dimensional freezing of laminar, fully developed Couette flow within an annular region with viscous dissipation. The solution is valid for small (at least an order of magnitude less than unity) but nonvanishing Stefan numbers. A translating outer sleeve induces the shear-driven motion in the liquid region. A closed-form expression for the instantaneous location of the solid–liquid interface is derived. In addition, expressions for the Nusselt number at the solid–liquid interface and dimensionless power (per unit length) are all derived as a function of pertinent dimensionless parameters. The analytical solution reduces to a few classical results in the appropriate asymptotic limits.

Problem Formulation

Shown in Fig. 1 is a one-dimensional region of thickness $(R_o - R_i)$. The motion of the liquid in the annular region, assumed to be laminar and fully developed, is shear driven by an outer cylinder or sleeve moving at constant speed V. The outer sleeve is modeled as

Received 24 December 1999; revision received 11 April 2000; accepted for publication 13 April 2000.

*Assistant Professor, Department of Mechanical Engineering; cahall@uno.edu. Member AIAA.

†Assistant Professor, Department of Mechanical Engineering.

‡Associate Professor, Department of Civil and Environmental Engineering.

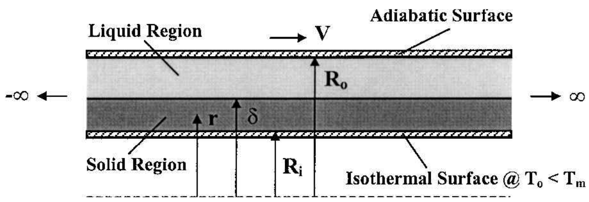

Fig. 1 One-dimensional model of annular Couette flow region undergoing solidification with translating outer sleeve.

an adiabatic surface, and the liquid is considered an incompressible, Newtonian fluid. The liquid is initially at or above its fusion temperature T_m according to a prescribed distribution $T_\ell = T_\ell(r, t < 0)$ and the inner cylinder is suddenly cooled isothermally to a temperature T_0 that is maintained below the liquid's fusion temperature. As a result, an axially symmetric freeze front propagates from the inner cylinder to the outer cylinder.

On introducing the following dimensionless parameters into the governing one-dimensional momentum and energy equations, including viscous dissipation,

$$\eta = \frac{r}{R_o}, \qquad \Delta = \frac{\delta}{R_o}, \qquad \beta = \frac{R_i}{R_o}, \qquad U = \frac{u}{V}$$

$$\theta = \frac{T - T_0}{T_m - T_0}, \qquad \tau = \frac{t}{R_o^2/\alpha_s}$$

$$Br = \frac{V^2 Pr}{c_\ell (T_m - T_0)} = \frac{\mu V^2}{k_\ell (T_m - T_0)}, \qquad Pr = \frac{\mu c_\ell}{k_\ell}$$

$$\gamma = \frac{k_\ell}{k_s}, \qquad Ste = \frac{c_s (T_m - T_0)}{h_{sf}} \tag{1}$$

where τ is the dimensionless time or Fourier number, Br is the Brinkman number, Pr is the Prandtl number, β is the annulus radius ratio, and Ste is the Stefan number, the solution for the velocity distribution in the liquid region can be derived as (assuming no-slip conditions at the solid–liquid interface)

$$U(\eta, \tau) = 1 - \frac{\ln(\eta)}{\ln[\Delta(\tau)]} \tag{2}$$

Subsequently, the solution $U(\eta, \tau)$ is used to determine the dimensionless temperature distribution in the liquid region via the dimensionless energy equation, that is,

$$\frac{1}{\eta}\frac{\mathrm{d}}{\mathrm{d}\eta}\left(\eta \frac{\mathrm{d}\theta_\ell}{\mathrm{d}\eta}\right) + Br\left(\frac{\partial U}{\partial \eta}\right)^2 = 0 \tag{3}$$

or, by using Eq. (2),

$$\frac{1}{\eta}\frac{\mathrm{d}}{\mathrm{d}\eta}\left(\eta \frac{\mathrm{d}\theta_\ell}{\mathrm{d}\eta}\right) + \frac{Br}{[\ln(\Delta)]^2}\frac{1}{\eta^2} = 0 \tag{4}$$

which is subject to the dimensionless boundary conditions

$$\left.\frac{\partial \theta_\ell}{\partial \eta}\right|_{\eta = 1} = 0, \qquad \theta_\ell(\eta = \Delta^+, \tau) = 1 \tag{5}$$

Integrating Eq. (4), subject to Eqs. (5), results in

$$\theta_\ell(\eta, \tau) = \frac{Br}{2[\ln(\Delta)]^2}[(\ln \Delta)^2 - (\ln \eta)^2] + 1 \tag{6}$$

The dimensionless one-dimensional temperature distribution in the solid region is governed by the heat diffusion equation, expressed in dimensionless form as

$$\frac{\partial \theta_s}{\partial \tau} = \frac{1}{\eta}\frac{\partial}{\partial \eta}\left(\eta \frac{\mathrm{d}\theta_s}{\mathrm{d}\eta}\right) \tag{7}$$

subject to the initial condition

$$\theta_s(\eta, \tau = 0) = \frac{Br}{2[\ln(\beta)]^2}[(\ln \beta)^2 - (\ln \eta)^2] + 1 \tag{8}$$

and boundary conditions

$$\theta_s(\eta = \beta, \tau) = 0, \qquad \theta_s(\eta = \Delta^-, \tau) = 1, \qquad \tau > 0 \tag{9}$$

The corresponding Stefan condition is given by[6]

$$\left.\frac{\partial \theta_s}{\partial \eta}\right|_{\eta = \Delta^-} - \gamma \left.\frac{\partial \theta_\ell}{\partial \eta}\right|_{\eta = \Delta^+} = \frac{1}{Ste}\frac{\mathrm{d}\Delta}{\mathrm{d}\tau} \tag{10}$$

An analytical solution to the present problem is possible when solidification is assumed to progress in a quasi-steady manner, which is valid when the Stefan number is small (at least an order of magnitude less than unity but nonvanishing). Therefore, the solution to the quasi-steady form of Eq. (7), subject to Eqs. (9), is

$$\theta_s(\eta, \tau) = \frac{\ln(\eta/\beta)}{\ln(\Delta/\beta)} \tag{11}$$

As a result, the Stefan condition becomes

$$\frac{1}{\ln(\Delta/\beta)} + \frac{\gamma Br}{\ln \Delta} = \frac{\Delta}{Ste}\frac{\mathrm{d}\Delta}{\mathrm{d}\tau} \tag{12}$$

which is cast in the following form,

$$\int_\beta^\Delta \frac{\Delta'(\ln \Delta')[\ln(\Delta'/\beta)]}{\ln \Delta' + \gamma Br \ln(\Delta'/\beta)}\,\mathrm{d}\Delta' = Ste \int_0^\tau \mathrm{d}\tau' \tag{13}$$

Integration of Eq. (13) gives the following analytical solution to the instantaneous freeze front location as a function of the dimensionless parameters γ, Br, β, and Ste:

$$\frac{1}{2(1 + \gamma Br)}\left[\Delta^2 \ln(\Delta/\beta) + (\Delta^2 - \beta^2)\left(\frac{\gamma Br \ln \beta}{1 + \gamma Br} - \frac{1}{2}\right)\right] - I(\Delta) = Ste \cdot \tau \tag{14}$$

where

$$I(\Delta) = K^2\left[\frac{\gamma Br(\ln \beta)^2}{(1 + \gamma Br)^3}\right]\left\{\ln\left[\frac{\ln(\Delta/K)}{\ln(\beta/K)}\right] + \sum_{j=1}^\infty \frac{2^j}{(j-1)!\, j^2} \times [\langle \ln(\Delta/K)\rangle^j - \langle \ln(\beta/K)\rangle^j]\right\} \tag{15}$$

$$K = \beta^{\gamma Br/(1 + \gamma Br)} \tag{16}$$

Note that as the freeze front moves toward the outer sleeve, the shear stress and, hence, the amount of viscous heating increases, which increases the liquid-side heat flux at the solid–liquid interface. Consequently, the solidification rate decreases and eventually becomes vanishingly small (steady state) when the liquid-side heat flux exactly balances the solid-side heat flux. This steady-state condition can be expressed mathematically as

$$1/\ln(\Delta_{ss}/\beta) + \gamma Br/\ln \Delta_{ss} = 0 \Rightarrow \Delta_{ss} = \beta^{\gamma Br/(1 + \gamma Br)} \tag{17}$$

which, incidentally, is equivalent to Eq. (16). Within the framework of the present model, there are some other quantities of interest, namely the Nusselt number at the freeze front, that is,

$$Nu = \frac{hR_o}{k_\ell} = \frac{\partial \theta_\ell}{\partial \eta}\bigg|_{\eta=\Delta^+} = \frac{-Br}{\Delta \ln \Delta} \tag{18}$$

and the power (per unit length L) required to maintain the sleeve in motion at constant speed, which is a function of the shear stress, given by

$$P = V\int \tau_{r=R_o}\,\mathrm{d}A = V(2\pi R_o L)\mu \frac{\partial u}{\partial r}\bigg|_{r=R_o} \Rightarrow P' = \frac{P}{L}$$

$$= 2\pi\mu V^2 \frac{\partial U}{\partial \eta}\bigg|_{\eta=1} \Rightarrow \frac{P'}{2\pi\mu V^2} = \frac{-1}{\ln \Delta} \tag{19}$$

It is observed that Eqs. (18) and (19) are related by

$$(\Delta/Br)Nu = P'/2\pi\mu V^2 = -1/\ln\Delta \tag{20}$$

and when Eq. (17) is substituted into Eq. (20) to obtain steady-state values, the following expression results:

$$\left(\frac{\Delta_{ss}}{Br}\right)Nu_{ss} = \left(\frac{P'}{2\pi\mu V^2}\right)_{ss} = \frac{-[1+(\gamma Br)^{-1}]}{\ln\beta} \tag{21}$$

Discussion

The closed-form solution given by Eq. (14) reduces to a few classical solutions when certain asymptotic limits are approached. For example, when the liquid medium is stationary everywhere ($Br \to 0$), the function I vanishes and the solution expressed by Eq. (14) reduces to

$$\tfrac{1}{2}\left[\Delta^2 \ln(\Delta/\beta) - \tfrac{1}{2}(\Delta^2 - \beta^2)\right] = Ste \cdot \tau \tag{22}$$

which is exactly the nondimensional form of the quasi-steady solution to outward freezing of a fluid in an annulus due to imposed temperature on the inner cylinder found in Ref. 6.

The solution given by Eq. (14) also reveals another asymptotic limit. As the freeze front location $\Delta \to K$, which is the steady-state condition expressed by Eq. (17), the function $I \to -\infty$ and the product $Ste \cdot \tau \to \infty$, which is consistent with the steady-state limit when the Stefan number is small but nonvanishing.

Figure 2 shows the temporal progression of the dimensionless freeze front location and Nusselt number at the freeze front for Brinkman numbers of 0 (stationary outer sleeve), 0.5, and 1. The liquid-to-solid thermal conductivity ratio is fixed at 0.4 and the annulus radius ratio is held at 0.3. Note that only the first two terms in the function I contribute appreciably to the solution expressed by Eq. (14). In Fig. 2, it is observed that the Brinkman number has a profound impact on the solidification rate. At zero Brinkman number, the freeze front location increases monotonically from 0.3 to unity. However, when the Brinkman number is increased to 0.5, solidification is delayed at early times due to liquid motion, although viscous heating effects are not yet significant. However, at latter times when $Ste \cdot \tau$ is greater than about 0.1, which is when viscous dissipation in the liquid dominates heat conduction in the solid, the solidification rate decreases and the freeze front location eventually reaches its steady-state value of $\Delta_{ss} = 0.818$ at about $Ste \cdot \tau = 1.06$. This is corroborated by the sharp increase in the interface Nusselt number when $Ste \cdot \tau > 0.1$. In fact, the interface Nusselt number increases from approximately 1.38 at early times to about 3.04 under steady-state conditions. A similar effect is observed when the Brinkman number is further increased to unity, although the steady-state interface location is lowered to about $\Delta_{ss} = 0.709$ due to an even further increase in viscous heating effects in the latter stages. For this case, the interface Nusselt number increases from its early

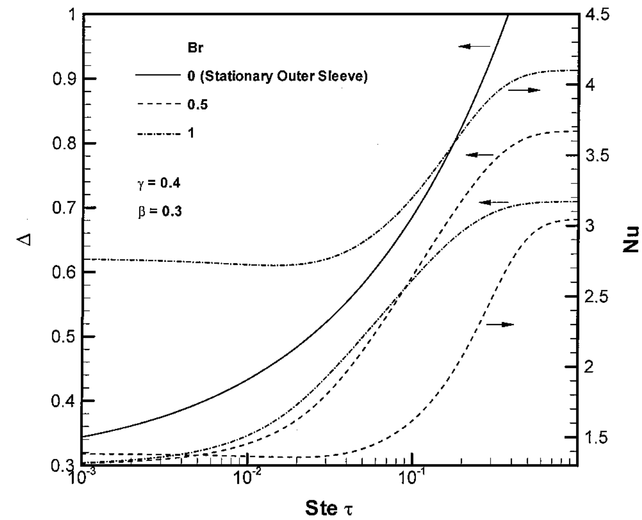

Fig. 2 Graphical representation of temporal variations in dimensionless freeze front location and interface Nusselt number for selected Brinkman numbers.

value of approximately 2.77 to its steady-state value of 4.1 at about $Ste \cdot \tau = 0.994$. Note that the Nusselt number line for $Br = 0$ is missing from Fig. 2 because the analysis reduces to a one-phase Stefan problem whereby the temperature remains uniform in the liquid because the outer surface is adiabatic.[6] Therefore, the heat flux on the liquid side (and, hence, Nusselt number) vanishes. As a result, all of the heat transfer from the annulus is divided amongst changing phase (latent heat removal) at the solid–liquid interface and sensibly cooling the solid. Furthermore, although not explicitly shown in Fig. 2, it is observed that the dimensionless power (per unit length) increases from 0.83 (initially) to 4.98 (steady state) and from 0.83 to 2.9 for Brinkman numbers of 0.5 and 1, respectively.

Conclusions

An analytical solution was presented for one-dimensional freezing of laminar, fully developed Couette flow within an annular region (with translating outer sleeve) for small but nonvanishing Stefan numbers. The effect of viscous dissipation in the liquid was taken into account. Closed-form expressions for the dimensionless instantaneous freeze front location, Nusselt number at the freeze front, dimensionless power (per unit length), and dimensionless steady-state freeze front location were derived as a function of liquid-to-solid thermal conductivity ratio, Brinkman number, annulus radius ratio, and the product of the Stefan and Fourier numbers. The analytical solution demonstrated that some classical results could be obtained in the appropriate asymptotic limits. The results also showed that the power requirements increased by a factor of up to five due to the solidifying annular Couette flow.

References

[1]Cheung, F. B., and Epstein, M., "Solidification and Melting in Fluid Flow," *Advances in Transport Processes*, edited by A. Mujumdar and R. A. Mashelkar, Wiley, New York, Vol. 3, 1984, pp. 35–117.

[2]Slocum, A. H., *Precision Machine Design*, Prentice–Hall, Englewood Cliffs, NJ, 1992, pp. 605–607.

[3]Bird, R. B., Stewart, W. E., and Lightfoot, E. N., *Transport Phenomena*, Wiley, New York, 1960, p. 68.

[4]Luelf, W. C., and Burmeister, L. C., "Viscous Dissipation Effect on Pressure Gradient for Laminar Flow of a Non-Newtonian Liquid Through a Duct of Subfreezing Wall Temperature," *Journal of Heat Transfer*, Vol. 118, No. 4, 1996, pp. 973–976.

[5]Huang, S. C., "Melting of Semi-Infinite Region with Viscous Heating," *International Journal of Heat and Mass Transfer*, Vol. 27, No. 8, 1984, pp. 1337–1343.

[6]Alexiades, V., and Solomon, A. D., *Mathematical Modeling of Melting and Freezing Processes*, Hemisphere, Washington, DC, 1993, pp. 47, 145.